ACS APPLIED MATERIALS & INTERFACES

Research Article

www.acsami.org

New Functional Amorphous Calcium Phosphate Nanocomposites by Enzyme-Assisted Biomineralization

Ee Taek Hwang,[†,‡,§] Rameshwar Tatavarty,[†,§] Jinyang Chung,[†] and Man Bock Gu*[,†]

[†]College of Life Sciences and Biotechnology, Korea University, Anam-dong, Seongbuk-Gu, Seoul, 136-701, South Korea

[‡]Institute of Bioprocess and Biosystems Engineering, Hamburg University of Technology, Denickestrasse 15, D-21073 Hamburg, Germany

ABSTRACT: In the present study, we report on enzyme-assisted formation of biomineralized amorphous calcium phosphate nanocomposites (ACP-NCs). About 100−200 nm sizes of the spherical porous enzyme-assisted ACP-NCs were successfully synthesized via double reverse microemulsion, but no ACP-NCs formed without the enzyme. It is believed that the enzyme was used as an organic template or additive that could regulate the biomineralization process. The enzyme-assisted ACP-NCs were well characterized by X-ray diffraction, transmission electron microscopy, scanning electron microscopy, dynamic light scattering, and Brunauer−Emmett−Teller (BET) criteria. The BET surface area, total pore volume, pore size from adsorption, and pore size from desorption of the ACP-NCs were 163 $m^2\ g^{-1}$ or 0.37 $cm^3\ g^{-1}$, 8.87 nm, and 7.48 nm, respectively. The enzyme-assisted ACP-NCs retained about 43% of the catalytic activity of free carboxyl esterase. Furthermore, they preserved their bioactivity even after the 10th reuse and were stable over 10 days even under a stringent shaking conditions. The reported method paves the way for novel biomineralization via enzyme molecules to form functional enzymes containing nanocomposites.

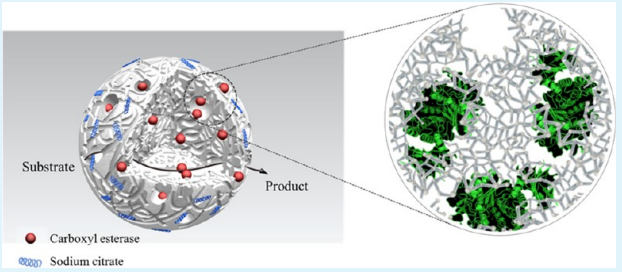

KEYWORDS: *enzyme, enzyme assisted biomineralization, bioinorganic nanocomposites, enzyme reuse, amorphous calcium phosphate, functional nanocomposites*

INTRODUCTION

Bioinspired mineralization for inorganic material synthesis, such as bone, crustacea, egg shell, and seashell, has drawn tremendous attention as a highly efficient and environmentally friendly process.[1−4] Recently, the morphology of the precipitate was reported to be affected by specific structure of an organic aggregation, especially in which the mineralization with a self-assembled organic molecule produced a unique inorganic structure.[5−7] For the first time, we have demonstrated that enzyme-assisted biomineralization and novel inorganic−organic biomineral structure with catalytic properties are derived from organic enzyme molecules.[8] By mimicking the formation of natural calcium phosphate, it has been found that the hard tissue contributes significantly to the biologically functionalized engineered materials with the rapid growth of nanotechnology.[9] Especially, the increasing evidence has shown that the phase of the amorphous calcium phosphate (ACP) plays a crucial role in the precipitation of calcium phosphate in a neutral solution with a suitable additive, such as a polymer, a charged adsorbing molecule, proteins, peptides, or amino acids.[9,10]

Since the amorphous calcium phosphate nanocomposites can be synthesized via either simple mixing or microemulsion formulation in wet chemical synthesis methods, the amorphous and porous nanocomposites thus obtained could be ideal nanocontainers. These biomolecules−nanocomposites have been engineered to form nanosized particles in the range of 20−300 nm.[11,12] The easy formation of biomineralized ACP have made them applicable eventually to the biomedicine field.[13−18] For example, they have been widely studied as delivery carriers of genes, siRNA, drugs, and flouro-phores.[13,14,19] A key feature of ACP nanocomposites is its intrinsic porosity that is useful for loading proteins, genes, drugs, etc.[20]

Considering the facts that the biomineralized ACP can be well formulated into nanoparticles, in the present study, we report successful fabrication and its feasibility of the biomineralized ACP-NCs assisted by enzyme molecules for the first time. About 100−200 nm sizes of the spherical porous ACP-NCs modulated by enzyme were successfully synthesized via double reverse microemulsion. These enzyme assisted ACP-NCs were characterized by using X-ray diffraction (XRD), transmission electron microscopy (TEM), scanning electron microscopy (SEM), dynamic light scattering (DLS), and Brunauer−Emmett−Teller (BET) to show the surface areas and their pore size distribution. The catalytic activity and stability of these enzyme-assisted ACP-NCs were also measured in vigorous shaking condition. Finally, the role of enzyme and the mechanism in these ACP-NCs assisted by enzymes were studied for understanding alternative biomineralization method for novel enzymatic applications.

Received: June 14, 2012
Accepted: December 31, 2012
Published: December 31, 2012

EXPERIMENTAL SECTION

Materials. Igepal CO-520 (Sigma, St. Louis, MO, USA), cyclohexane (99%, Sigma), *N*,*N*-dimethylformamide (99.8%, Sigma), calcium chloride dihyride (Sigma), *p*-nitrophenyl butyrate (Sigma), and sodium phosphate dibasic (Sigma) were purchased and used without any additional purification. Alcohol dehydrogenase from baker's yeast (Sigma), α-chymotrypsin from bovine pancreas, peroxidase type II from horseradish, and carboxyl esterase from *Rhyzopus oryzae* (Biochemik Chemicals) were purchased from Sigma and used in the biomineralization process. BCA Protein Assay kit (Pierce, Rockford, IL, USA) was used to measure enzyme concentrations following the manufacturer's protocol.

Synthesis of Enzyme-Assisted ACP-NCs. The enzyme-assisted ACP-NCs were synthesized via a well-known double-reverse microemulsion procedure as reported previously.[15] In brief, separate 10 mL glass vials with an aqueous phase of 120 μL of (A) 100 mM calcium chloride and (B) 100 μL of 60 mM disodium hydrogen phosphate containing 20−100 μL of varying amounts of carboxyl esterase enzyme (10−50 mg mL^{-1}) were added to 2.65 mL of cyclohexane containing 30 vol % of Igepal CO-520 and stirred at high speed (600 rpm) for 20 min to obtain clear microemulsions of A and B. Next, microemulsion B, containing enzyme, was slowly dropped into microemulsion A and stirred for 5 min to completely mix both emulsions and allow for the formation of a calcium phosphate precipitate in the nanosized droplets of the microemulsion. Then, 50 μL of sodium citrate (15 mM) was added to the microemulsion to stabilize the amorphous calcium phosphate nanocomposites and further reacted for 20 min. The emulsion was disrupted by adding three times the volume of ethanol, and a clear white fluffy precipitate of amorphous calcium phosphate particles was seen. The solution was centrifuged at 6000 rpm, washed three to four times with ethanol and water, vacuum-dried, and stored as a dry powder until further use. The entrapped enzyme loading capacity was measured using a BCA protein assay kit.

Characterization of the Enzyme-Assisted ACP-NCs. The XRD patterns were obtained using a PW 3830 X-ray generator and Ni-filtered Cu Kα radiation. Intensity data were collected over a 2θ range of 20−80° with a 0.02° step size using a counting time of 0.1 s per point. TEM (Tecnai 12, Philips, Eithoven, The Netherlands) was used for obtaining the high resolution imaging of enzyme-assisted ACP-NCs dispersed in distilled water and dropped onto a carbon supported 300 mesh copper specimen grid. Imaging was done at 100 keV to avoid beam damage to the enzyme-assisted biomineralized nanocomposites. A particle size analysis was carried out by DLS using Malvern Instruments nanocomposite size analyzer (NanoZS, Worcestershire, UK). The hydrodynamic diameter of the enzyme-encapsulated nanocomposites was measured by dissolving 1 mg of dry nanocomposite powder per 1 mL of distilled water. The morphology and elemental analysis of the enzyme-assisted ACP-NCs were investigated by SEM (S-2360N equipped with energy-dispersive X-ray spectroscopy (EDAX) (Hitachi Co. Ltd., Tokyo, Japan). BET surface area and pore size analyses were conducted using a Micromeritics instrument (Tristar 3020). Pore-size distributions were calculated using the Barett−Joyner−Halenda (BJH) method.

ACP-NCs Esterase Activity Measurement and Reuse in the Hydrolysis Reaction. The bioactivity of 1 mg of enzyme-assisted ACP-NCs was measured by monitoring the production of *p*-nitrophenol from the hydrolysis of *p*-nitrophenyl butyrate dissolved in *N*,*N*-dimethylformamide. In brief, 1.98 mL of 100 mM phosphate buffer (pH 6.5) containing 20 μL of 50 mM *p*-nitrophenyl butyrate dissolved in *N*,*N*-dimethylformamide was prepared as a substrate. The ACP-NCs were dispersed in this substrate solution and shaken at 200 rpm. After a short reaction, initial activity was measured by absorbance changes at 400 nm with time, and the absorbance was converted to a standard curve of *p*-nitrophenol concentrations. For reuse experiments, ACP-NCs were washed with 100 mM phosphate buffer (pH 6.5) three times and stored at room temperature for further use under a stringent shaking condition at 200 rpm. The same experimental protocol was used when we measured ACP-NC activity during repeated use. One unit (U) of carboxyl esterase activity was defined as the amount of enzyme releasing 1 μmol *p*-nitrophenol per minute under assay conditions. All samples were measured in triplicate for error analysis. The standard deviations are shown as error bars within the graphs.

RESULTS AND DISCUSSION

Physicochemical Characteristics of Enzyme-Assisted Biomineralized ACP-NCs. Fabrication of the ACP-NCs was successfully modulated by the enzyme carboxyl esterase (CE). The synthesis of these ACP-NCs was carried as previously reported for preparing a simple double reverse microemulsion,[12] but no ACP-NCs formed without the enzyme. These enzyme-assisted biomineralized ACP-NCs with a porous structure are depicted in Scheme 1. It is believed that the enzyme could be used as an organic template or additive that could regulate the biomineralization process in this study. We presume that the biomineralization process to form ACP with a porous structure was due to the interaction of calcium and phosphate ions with amino and carboxyl group residues of the enzyme in the water-in-oil emulsion stabilized by the IGEPAL CO-520 surfactant. Once the amorphous calcium phosphate nanocomposites formed, they were further stabilized by sodium citrate to make the particles water dispersible and inhibit the nucleation and/or growth due to citrate binding onto active growth sites of the newly formed nuclei.[21] In such a scenario, growth of the nuclei was inhibited until there was sufficient supersaturation of calcium in solution for precipitation to occur. Some studies have found that the presence of citrate delays the occurrence of crystals and reduces the crystallization rate, which slows down the transformation of these particles into a more stable calcium phosphate form.[22]

Scheme 1. Schematic Illustration of Biomineralized Amorphous Calcium Phosphate Nanocomposites (ACP-NCs) Showing Formation of ACP-NCs via an Entrapment of Enzyme

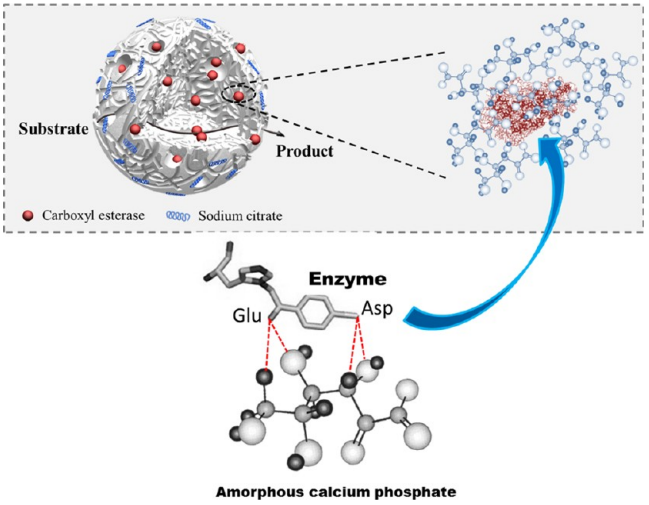

In order to show the effects of different enzymes on the morphological changes during the formation of ACP-NCs, glucose oxidase, alcohol dehydrogenase, and chymotrypsin, which are frequently utilized via immobilization onto the porous materials as representative biocatalysts in chemical synthesis and industrial applications,[23] was tested in this study. As shown in Figure 1b−d, each enzyme induced different morphologies which can be seen in tree shaping showing

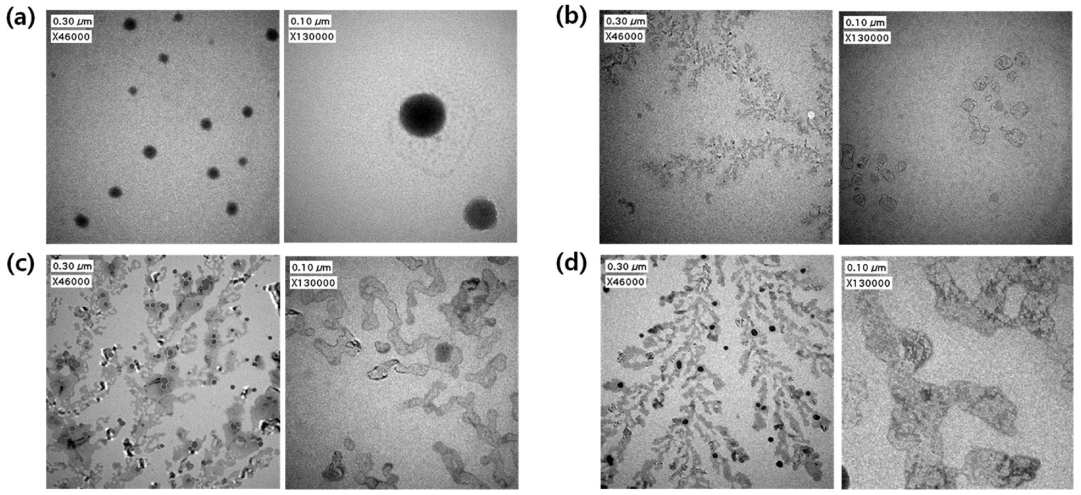

Figure 1. Representative transmission electron micrograph (TEM) images of enzyme-assisted amorphous calcium phosphate nanocomposites (ACP-NCs) obtained when various enzymes were used in the microemulsion synthetic procedure, (a) carboxyl esterase, (b) glucose oxidase, (c) alcohol dehydrogenase, and (d) chymotrypsin, respectively.

tripinnatisect, lobate, and pinnatisect, respectively. These changes were attributed to the different PIs, amino acid residues, rigidity, and three-dimensional structure of each enzyme used as a template during biomineralization. In addition, the different experimental conditions in the double-reverse microemulsion method also affected ACP-NCs formation. In fact, several parameters, such as the concentrations of calcium and phosphate ions, ionic strength, pH, temperature, and the concentration of surfactants, were known to play an important role on the size and morphologies of the calcium phosphate nanoparticles.[24] Especially, the previous study reported the ionic strength of the surfactants influence the size and the morphology change.[25] Since the carboxyl esterase is widely used in many different industrial processes including a chiral building block drug synthesis in an organic solvent,[26,27] it has been specifically focused to make uniform spherical biomineralized nanocomposites in this study.

The fabricated enzyme-assisted ACP-NCs were successfully characterized by XRD patterns, TEM, DLS, pore-size-distribution analysis, SEM, BET surface area, pore size analysis, and elemental analysis. No discernible peaks of crystalline calcium phosphate were observed in the XRD pattern, but characteristic data, $2\theta = 30°$, indicating the amorphous nature of the calcium phosphate nanocomposites, were obtained (Figure 2a). The TEM images of the enzyme-assisted ACP-NCs showed uniform spherical nanospheres of about 100−200 nm (Figure 2b), and no precipitation of ACP was observed without enzyme. The particle size distribution obtained by DLS concurred with the TEM images (Figure 2c).

A key feature of the ACP-NCs the previous studies were their porosity, which is highly desirable for drug or protein loading.[28] In this study, these enzyme-assisted ACP-NCs synthesized are also expected to have pore sizes large enough for small molecules to pass through without limitation. In fact, the representative nitrogen adsorption/desorption isotherms along with the corresponding pore-size distributions were obtained from the N_2 adsorption data using the BJH method. The presence of these pores (7−9 nm) in the enzyme-assisted ACP-NCs is also clearly shown in Figure 3. The BET surface area and single-point total pore volume of the enzyme-assisted ACP-NCs were 163 $m^2\ g^{-1}$ and 0.37 $cm^3\ g^{-1}$, respectively. These unique characteristics offer several favorable biocatalyst

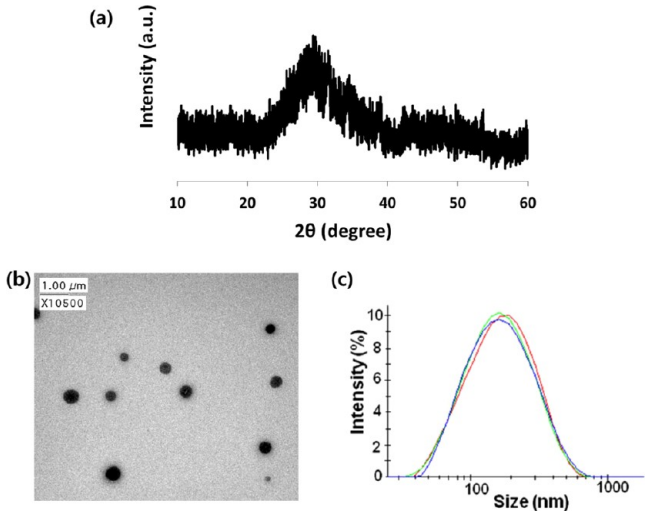

Figure 2. Characterization of amorphous calcium phosphate nanocomposites (ACP-NCs) prepared in this study, (a) X-ray diffraction patterns, (b) transmission electron micrograph images of ACP-NCs, and (c) particle size distribution of ACP-NCs.

features. It is anticipated that a proper size of nanocomposites would be desirable, because they can accommodate large as well as an increased number of pores, leading to efficient diffusion of substrate in and product out from the surface of the nanocomposites.

The elemental composition of these enzyme-assisted ACP-NCs was analyzed to be its atomic ratio of Ca:P, 1.41:1.24, measured by energy-dispersive X-ray spectroscopy (EDAX) and found to contain various elemental peaks corresponding to carbon, oxygen, calcium, and phosphate, respectively (Figure 4). The ratio of Ca:P was low, compared to the synthesis ratio (1.35:1) in another report.[29] This seems to be likely due to the formation of calcium−enzyme complexes which are excluded from the particle during the biomineralization.[15] In addition, the ratio of organic:inorganic was found to be 1.30:1.00, and the high organic ratio content must be due to citrate coating and enzyme composition.

Reuse of Enzyme-Assisted Biomineralized ACP-NCs. We hypothesize that the enzymes entrapped in the ACP-NCs

dx.doi.org/10.1021/am302580p | ACS Appl. Mater. Interfaces 2013, 5, 532−537

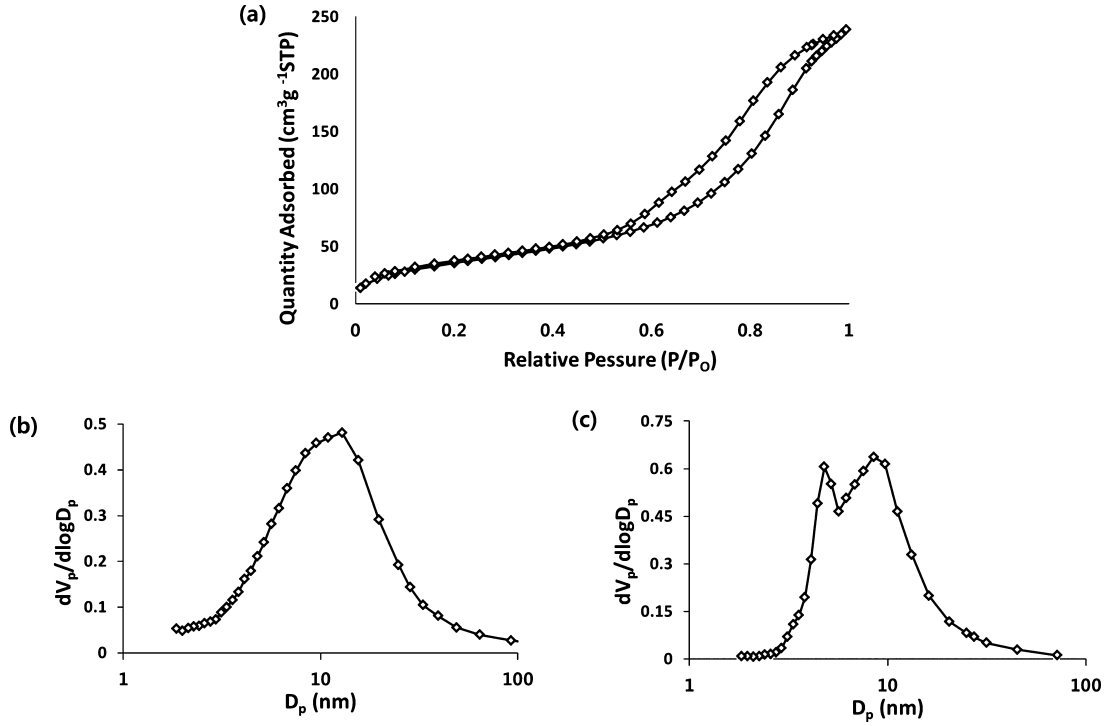

Figure 3. Characterization of ACP-NCs by (a) N_2 adsorption−desorption isotherms and pore size distributions from (b) adsorption and (c) desorption.

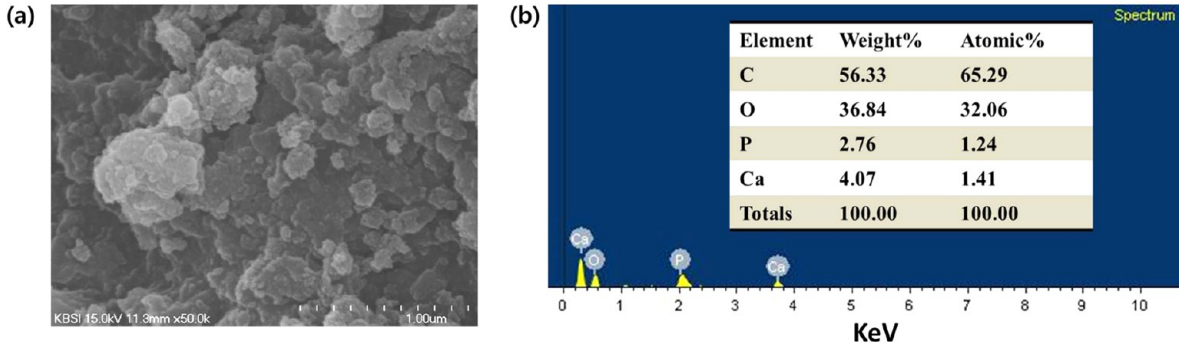

Figure 4. Scanning electron microscopy (SEM) image and energy-dispersive X-ray spectroscopy (EDAX) analysis of enzyme-assisted amorphous calcium phosphate nanocomposites (ACP-NCs). The blowup of SEM image shows the small, individual enzyme-assisted ACP-NCs aggregates with sizes <100 nm.

would not be leached out, leading to high enzyme loading with concomitant improved stabilization of the enzyme activity. It was found that the entrapment of CE enzyme was completed in less than 30 min. In the mineralization process, if the enzyme concentration is varied, the entrapped amounts of the enzyme came to be changed, and so the amounts of ACP-NCs are changed as well. In other words, unless the ratios of enzyme and calcium and phosphate ions are not maintained constant as the amount of enzyme is changed, then some are not entrapped. In fact, these experimental conditions were successfully optimized for the highest specific activity. Therefore, in this study, the highest enzyme loading condition is obtained for the formation of the enzyme-assisted ACP-NCs, as shown in Figure 5. First, 0.5 mg of enzyme was used in the biomineralization process, and then, ACP-NCs were washed and dried to remove all enzymes which were not entrapped. To measure a concentration of entrapped enzyme, the ACP-NCs were treated with a chemical agent, ethylenediaminetetraacetic

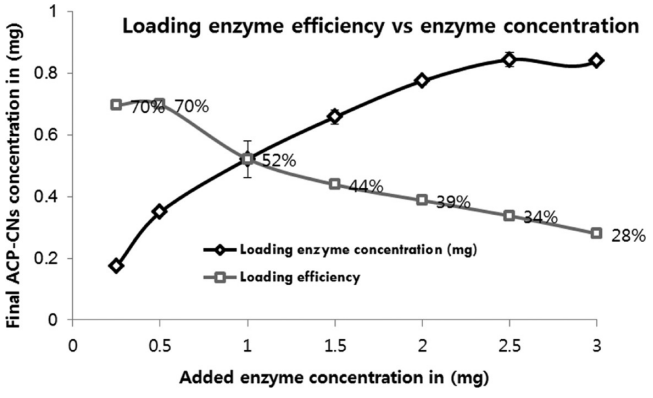

Figure 5. Enzyme loading efficiency of ACP-NCs according to varying enzyme concentrations.

acid, to dissolve them, and the enzyme concentration was estimated to be 0.35 mg from the micro BCA protein assay test,

dx.doi.org/10.1021/am302580p | ACS Appl. Mater. Interfaces 2013, 5, 532−537

indicating that 70% of free enzyme (0.5 mg) was the theoretical maximum value.

After enzyme-assisted biomineralization, the specific activities of free CE and ACP-NCs were measured to be 1.20 and 0.51 μM s^{-1} per mg of CE, respectively, as shown in Figure 6. In

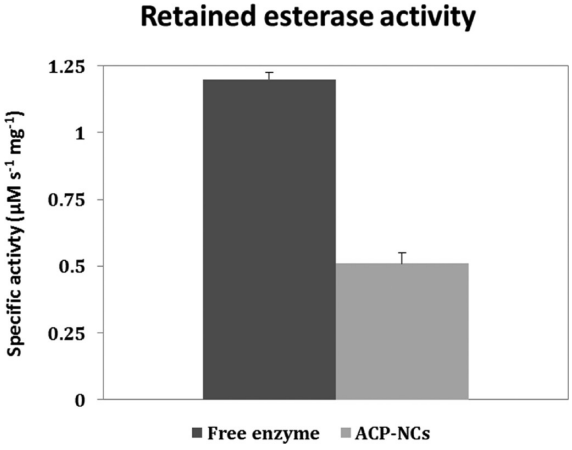

Figure 6. Retained esterase activity of the ACP-NCs after biomineralization.

other words, the specific activity of ACP-NCs was calculated to be 43% of the free CE's specific activity. The enzyme kinetics was determined and compared to that of the free enzyme as listed in Table 1. Only a small change in the K_m value was seen

Table 1. Summary of Lineweaver–Burk Plots for the Free Enzyme and the ACP-NCs

	k_m [μM]	V_{max} [μM s^{-1}]
free enzyme	858	3.397
ACP-NCs	928	1.284

when compared to that of the free enzyme (Table 1). As shown in Table 1, the decrease in V_{max} can be interpreted as reduced enzyme flexibility for catalysis, due to the multipoint attachment between the amino acid residues in each enzyme molecule and the Ca^{2+} and PO_4^{3-} anions of the ACP-NCs.[8,30,31] However, the apparent binding constant (K_m) of the enzyme-assisted ACP-NCs was nearly the same as that of the free enzyme. This suggests that the precipitated amorphous calcium phosphate structure did not cause a large mass-transfer limitation for the substrate, which was likely due to its large sized pores.

Prevention of enzyme leaching from the ACP-NCs is accompanied with improved enzyme stability and these effects were investigated. The stabilities of the free CE and ACP-NCs were evaluated by incubating them in aqueous buffer under shaking conditions (200 rpm), to mimic natural environments occurring in enzyme reactor studies. In a typical industrial enzymatic process setup, harsh shaking conditions are involved and it is highly desirable to maintain the stability of enzyme under such conditions. The initial esterase activity of the ACP-NCs is assumed to be 100%, as the relative esterase activity of ACP-NCs was defined as the ratio of the activity to that of the initial enzyme activity. As shown in Figures 7 and 8, the ACP-NCs showed high stability without any loss of catalytic activity under stringent shaking conditions (200 rpm). The ACP-NCs preserved >85% of their initial catalytic activity, even after 10

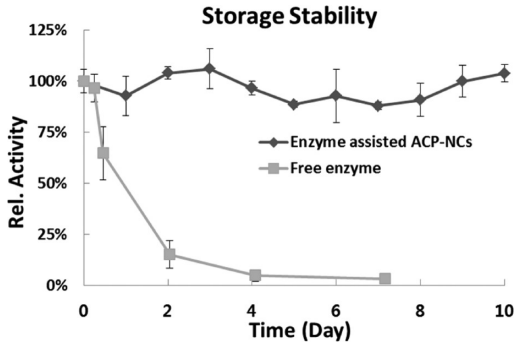

Figure 7. Storage stability of the ACP-NCs in the hydrolysis reaction, ACP-NCs were kept under rigorous shaking conditions of 200 rpm, and relative activity was calculated using the residual activity at each use, relative to that found initially on its first use.

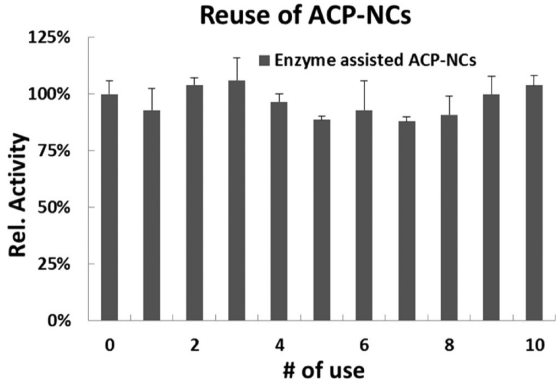

Figure 8. Reuse of the ACP-NCs in the hydrolysis reaction (relative activity was calculated using the residual activity at each use, relative to that found initially on first use).

reuses, over 10 days. The ACP-NCs showed excellent recycling and storage stability under rigorous shaking conditions, as depicted in Figures 7 and 8. In comparison with the other previous studies,[32] in which enzymes were immobilized with different nanomaterials, such as polymeric nanofibers, nanoparticles, carbon nantubes, or mesoporous silica, this study showed high retention of activity and stability. Those other methods employed enzyme coating on the surface of materials or enzyme entrapment inside of materials by using a glutaraldehyde (GA) based cross-linking technique. In addition, the nanomaterials were synthesized in advance, and then utilized for enzyme immobilization. However, in this study, ACP-NCs enable highly stable enzyme entrapment inside the nanoparticles with formation of their composites, simultaneously without any GA treatment. The high stability of the enzyme-assisted ACP-NCs occurred due to the interaction of the amino acids Glu and Asp in the enzyme with calcium phosphate species and their wide distribution within the amorphous calcium phosphate matrix.[31,33] Furthermore, the ACP-NCs were separated by centrifugation and resuspended in distilled water for the next use, which allowed easy separation from the reaction medium. The two ionized carboxyl groups in the amino acids interacted with Ca^{2+} and the phosphate anions interacted with the protonated amino group ($-NH_3^+$). This amino acid residue interacting mechanism enhanced stability of the ACP-NCs and induced formation of stable and unique ACP-NCs. This is the first report on the feasibility of enzyme-assisted ACP-NCs. As a model, these ACP-NCs could be

further modified with polymeric ligands for control of their morphology and as a novel application for enzymatic processes.

CONCLUSIONS

ACP-NCs were successfully fabricated by enzyme-assisted biomineralization and were found to be novel nanocomposites in terms of enzyme stability and reusability. The ACP-NCs were successfully characterized by X-ray diffraction, transmission electron microscopy, scanning electron microscopy, dynamic light scattering, BET surface area, pore size analysis, and energy-dispersive X-ray spectroscopy (EDAX) analysis. The ACP-NCs composites showed high enzyme loading capacity up to ~70%. They were highly stable and retained up to 85% of their relative enzyme activity even after 10 reuses under very harsh shaking conditions. In addition, the enzyme was easy to load and separate via precipitation.

AUTHOR INFORMATION

Corresponding Author

*Phone: +82-2-3290-3417. Fax: +82-2-928-3555. E-mail: mbgu@korea.ac.kr.

Author Contributions

§These authors contributed equally.

Notes

The authors declare no competing financial interest.

ACKNOWLEDGMENTS

This work was supported by a National Research Foundation of Korea Grant funded by the Korean Government (MEST) (NRF-C1ABA001-2010-0020501) .

REFERENCES

(1) Shen, X. Y.; Belcher, A. M.; Hansma, P. K.; Stucky, G. D.; Morse, D. E. *J. Biol. Chem.* **1997**, *272*, 32472−32481.
(2) Lowenstam, H. A. *Science* **1981**, *211*, 1126−1131.
(3) Mann, S. *Nature* **1993**, *365*, 499−505.
(4) Stupp, S. I.; Braun, P. V. *Science* **1997**, *277*, 1242−1248.
(5) Guo, X. H.; Yu, S. H. *Cryst. Growth Des.* **2007**, *7*, 354−359.
(6) Shi, Y.; Zhang, Y. H.; Yang, W. L.; Tang, Y. *Chem. Commun.* **2009**, *4*, 442−444.
(7) Cai, Y. R.; Tang, R. K. *J. Mater. Chem.* **2008**, *18*, 3775−3787.
(8) Hwang, E. T.; Gang, H.; Chung, J.; Gu, M. B. *Green Chem.* **2012**, *14*, 2216−2220.
(9) Tang, R. K.; Darragh, M.; Orme, C. A.; Guan, X. Y.; Hoyer, J. R.; Nancollas, G. H. *Angew. Chem., Int. Ed.* **2005**, *44*, 3698−3702.
(10) Klesing, J.; Wiehe, A.; Gitter, B.; Grafe, S.; Epple, M. *J. Mater. Sci-Mater. M.* **2010**, *21*, 887−892.
(11) Klesing, J.; Chernousova, S.; Kovtun, A.; Neumann, S.; Ruiz, L.; Gonzalez-Calbet, J. M.; Vallet-Regi, M.; Heumann, R.; Epple, M. *J. Mater. Chem.* **2010**, *20*, 6144−6148.
(12) Sokolova, V.; Epple, M. *Angew. Chem., Int. Ed.* **2008**, *47*, 1382−1395.
(13) Li, J.; Chen, Y. C.; Tseng, Y. C.; Mozumdar, S.; Huang, L. *J. Controlled Release* **2010**, *142*, 416−421.
(14) Mukesh, U.; Kulkarni, V.; Tushar, R.; Murthy, R. S. R. *J. Biomed. Nanotechnol.* **2009**, *5*, 99−105.
(15) Morgan, T. T.; Muddana, H. S.; Altinoglu, E. I.; Rouse, S. M.; Tabakovic, A.; Tabouillot, T.; Russin, T. J.; Shanmugavelandy, S. S.; Butler, P. J.; Eklund, P. C.; Yun, J. K.; Kester, M.; Adair, J. H. *Nano Lett.* **2008**, *8*, 4108−4115.
(16) Altinoglu, E. I.; Russin, T. J.; Kaiser, J. M.; Barth, B. M.; Eklund, P. C.; Kester, M.; Adair, J. H. *ACS Nano* **2008**, *2*, 2075−2084.
(17) Sokolova, V. V.; Radtke, I.; Heumann, R.; Epple, M. *Biomaterials* **2006**, *27*, 3147−3153.
(18) Bisht, S.; Bhakta, G.; Mitra, S.; Maitra, A. *Int. J. Pharm.* **2005**, *288*, 157−168.
(19) Zhang, M. Z.; Kataoka, K. *Nano Today* **2009**, *4*, 508−517.
(20) Epple, M.; Ganesan, K.; Heumann, R.; Klesing, J.; Kovtun, A.; Neumann, S.; Sokolova, V. *J. Mater. Chem.* **2010**, *20*, 18−23.
(21) Giocondi, J. L.; El-Dasher, B. S.; Nancollas, G. N.; Orme, C. A. *Philos. Trans R. Soc. A.* **2010**, *368*, 1937−1961.
(22) Lei, C. H.; Shin, Y. S.; Liu, J.; Ackerman, E. J. *J. Am. Chem. Soc.* **2002**, *124*, 11242−11243.
(23) Hartmann, M.; Jung, D. *J. Mater. Chem.* **2010**, *20*, 844−857.
(24) Montastrue, L.; Azzaro-Pantel, C.; Biscans, B.; Cabassud, M.; Bomenech, S. *Chem. Eng. J.* **2003**, *94*, 41−50.
(25) Singh, S.; Bhardwaj, P.; Singh, V.; Aggarwal, S.; Mandal, U. K. *J. Colloid Interface Sci.* **2008**, *319*, 322−329.
(26) Van der Houwen, J. A. M.; Cressey, G.; Cressey, B. A.; Valsami-Jones, E. *J. Cryst. Growth* **2003**, *249*, 572−583.
(27) Sheldon, R. A. *Org. Process Res. Dev.* **2011**, *15*, 213−223.
(28) Pamies, O.; Backvall, J. E. *Trends Biotechnol.* **2004**, *22*, 130−135.
(29) Combes, C.; Rey, C. *Acta Biomater.* **2010**, *6*, 3362−3378.
(30) Kim, J.; Grate, J. W. *Nano Lett.* **2003**, *3*, 1219−1222.
(31) Ikawa, N.; Kimura, T.; Oumi, Y.; Sano, T. *J. Mater. Chem.* **2009**, *19*, 4906−4913.
(32) Kim, J.; Grate, J. W.; Wang, P. *Chem. Eng. Sci.* **2006**, *61*, 1017−1026.
(33) Espanol, M.; Perez, R. A.; Montufar, E. B.; Marichal, C.; Sacco, A.; Ginebra, M. P. *Acta Biomater.* **2009**, *5*, 2752−2762.